World Academics Journal of Engineering Sciences
Vol.**11**, Issue.**1**, pp.**07-15**, March **2024**
E-ISSN: 2348-635X
Available online at: www.isroset.org

Research Article

Electric Field Modulation and Thermal Radiation in Mathematical Models of Blood Flow for Breast Cancer Therapy

Adamu Garba Tahiru[1], Isah Abdullahi[2*], Idris Babaji Muhammad[3], Mahmood Abdulhameed[4], Mukhtar Abubakar Maiwada[5]

[1,3,5]Dept. of Mathematical Sciences, Bauchi State University, Gadau, Bauchi, Nigeria
[2]Dept. of Mathematical Sciences, Abubakar Tafawa Balewa University, Bauchi, Nigeria
[4]Dept. of Electrical &Electronics Engineering, Abubakar Tafawa Balewa University, Bauchi, Nigeria

**Corresponding Author's: isahabdullahi7474@gmail.com, Tel: +2347039747474*

Received: 18/Dec/2023; **Accepted**: 20/Jan/2024; **Published**: 31/Mar/2024

Abstract—In this research work, we try to provides a comprehensive overview of research related to blood flow in the circulatory system, with a focus on the application of mathematical models to study arterial blood flow under the influence of a magnetic field. It discusses the importance of understanding blood flow for therapeutic interventions, particularly in the context of cancer treatment and drug delivery to cancer cell membranes. The impact of cardiovascular diseases on human health is highlighted, emphasizing the significance of studying the circulatory system and blood flow for advancing treatments for conditions such as hypertension and myocardial infarction. The integration of mathematical models is presented as a valuable tool for simulating and understanding the complexities of blood flow, leading to potential advancements in therapeutic interventions. The study also addresses the influence of various factors such as thermal radiation, magnetic nanoparticles, electric field, and radiation parameter on magneto-hydrodynamic blood flow, particularly in the context of breast cancer treatment. Additionally, it discusses the potential applications of mass transfer for drug delivery and clinical administration. The research aims to contribute to the diagnosis and treatment of breast cancer and other cardiovascular diseases, aligning with broader efforts to understand the behavior of magneto-hydrodynamic blood flow in the cardiovascular system. From the findings, it can be concluded by emphasizing the importance of understanding blood flow and its impact on human health, particularly in the context of therapeutic development and the treatment of cardiovascular diseases, while also highlighting promising avenues for future research and therapeutic advancements.

Keywords— Nanoparticles, Electric Field, Thermal Radiation, Breast Cancer

1. Introduction

The human circulatory system relies on the rhythmic contractions of the heart, creating a pulsatile pressure gradient throughout the system. This physiological blood flow is crucial for delivering drugs to tumor cell membranes and initiating chemical reactions between tumors and circulating fluids. Achieving a biologically compatible reaction rate holds promise for therapeutic development. However, despite blood's essential roles, significant human losses persist due to various cardiovascular diseases, including hypertension, cerebral strokes, angina pectoris, myocardial infarction, and cancer, occurring at different locations within the cardiovascular system under disease conditions. Despite available treatments like surgery, radiotherapy, chemotherapy, and immune therapy, a substantial gap remains in addressing human losses, particularly in cancer [1].

In the pursuit of understanding blood flow, numerous mathematical models have been developed to investigate arterial blood flow under the influence of a magnetic field. For example, [2,3,4] have contributed to this field. The study of magneto-hydrodynamic (MHD) blood flow in arteries has gained considerable attention due to its diverse applications in medical and physiological fields. Recent mathematical models have specifically focused on exploring the flow behaviour of blood for various non-Newtonian fluids. [5,6] analysed pulsatile blood flow using the Casson non-Newtonian fluid model. [7] investigated the unsteady and incompressible arterial blood flow of non-Newtonian fluid, particularly micro-polar fluid, through a composite artery. Additionally, [8] researched the influence of the magnetic field on non-Newtonian blood flowing through an artery with a stenosis, emphasizing wall-slip conditions. The study considered the effect of the Lorentz force, revealing its considerable opposition to blood motion in electrically conducting conditions. Consequently, the application of a

magnetic field led to a decrease in velocity and shear stress at the wall. [9] conducted an investigation into the influence of both heat sources and a magnetic field on blood flow within a bifurcated artery. Their study encompassed various flow parameters, including temperature distribution, axial and normal velocities, and these were systematically examined in relation to magnetic field strength, heat source parameter, and Prandtl number. The outcomes of their research revealed a significant impact of the magnetic field on the flow pattern, suggesting potential applications for hypertension treatment. Additionally, they observed that the heat source had the effect of increasing blood temperature, indicating potential applications in thermal therapy for tumor.

In related studies, [10,11] explored the application of heat sources and chemical reactions in magneto-hydrodynamic blood flow through permeable bifurcated arteries with an inclined magnetic field, with a particular focus on tumor treatments. They employed analytical methods, utilizing the undetermined coefficient technique to solve the governing equations. Their results indicated that addressing high blood pressure concerns, in conjunction with appropriate clinical administration and tumor cell permeability, could be effectively achieved. The researchers concluded that mass transfer represents a promising approach for drug delivery and clinical administration.

Building upon these recent investigations but taking a different approach, the current research adopts an electro-magneto-hydrodynamic approach to blood flow in small slip arteries. Inspired by the work of [10,11,12], the studies place specific emphasis on comprehending the effects of thermal radiation, Magnetic Nanoparticles, and the electric field in magneto-hydrodynamic blood flow through small slip arteries with an inclined magnetic field, specifically for breast cancer treatment. The motivation behind this exploration lies in the numerous potential applications for drug delivery to cancer cells and mass transfer. This research aligns with broader efforts aimed at understanding the behaviour of magneto-hydrodynamic blood flow in the cardiovascular system, undertaken by various researchers using either experimental or theoretical approaches, with the overarching goal of contributing to the diagnosis and treatment of breast cancer and other diverse cardiovascular diseases

2. Related Work

To exemplify, the investigation into the arterial impact of a magnetic field by [10,11,12] has conclusively demonstrated that the application of a magnetic field holds considerable potential for effectively regulating both blood flow and pressure. Notably, these studies underscored the magnetic field's influence on flow patterns. Through the utilization of analytical solutions to the equations of motion, the researchers delved into the effects of the Prandtl number and magnetic field on the flow. It is imperative to build upon these findings, and this study is specifically geared towards enhancing the existing model proposed by [12]. This enhancement entails incorporating additional factors, namely the effects of an electric field, Nanoparticles, and Thermal radiation on blood velocity and temperature, aspects that were not addressed in the previous work.

Considering the slight electrical conductivity of human blood, a critical aspect of this study involves the modification of a mathematical model to accurately replicate the influence of the electric field in electro-magneto-hydrodynamic blood flow through small slip arteries with an inclined magnetic field. This modification serves the purpose of facilitating the observation of various physiological parameters, some of which cannot be directly obtained through experimental investigations. In the context of this study, blood is conceptualized as a non-Newtonian, compressible, heterogeneous, and viscous fluid flowing in a non-conductive parallel plate channel.

This research endeavour extends the insights gained from [10,11,12], providing a nuanced understanding of the intricate interplay between magnetic, electric, and thermal influences on blood flow within specific arterial conditions. By expanding the existing model, this study aims to contribute significantly to the comprehension of electro-magneto-hydrodynamic blood flow, offering valuable insights that could potentially have implications for the diagnosis and treatment of cardiovascular diseases, with a particular focus on breast cancer. The inclusion of additional factors such as Nanoparticles and Thermal radiation represents a novel approach, addressing gaps in the previous research and paving the way for a more comprehensive understanding of the complex dynamics involved in the circulatory system under the influence of external fields.

3. Methodology

The equation that dictates the connection between shear stress and strain rate in an incompressible flow of a Casson fluid is formulated as follows [13,14]:

$$\tau_{ij} = \begin{cases} 2\left(\mu_B + \dfrac{\tau_y}{\sqrt{2\pi}}\right)\ell_{ij}; \pi > \pi_c \\ 2\left(\mu_B + \dfrac{\tau_y}{\sqrt{2\pi_c}}\right)\ell_{ij}; \pi > \pi_c \end{cases} \quad (1)$$

The parameters in this context are defined as follows: $\pi = \ell_{ij}\ell_{ij}$ and ℓ_{ij} represents the the (i,j)-th constituent of the deformation rate, μ_B representing plastic dynamic viscosity, while τ_y signifies fluid yield stress, and π results from multiplying the deformation rate by itself. The critical value of this product, based on the non-Newtonian model, is denoted as π_c. The primary emphasis is on the Casson fluid model rather than the Papanastasiou-Casson regularization model, with the former being a more recent approach. The validation of current findings is supported by extensive research on the Casson fluid model over the past few decades. The Casson fluid model is recognized for its simplicity compared to the Papanastasiou-Casson regularization model,

leading many researchers to choose numerical investigations of the latter due to its complexity. Given the analytical approach in this study, the Casson fluid model is considered imperative. The governing equations for the problem, in line with Boussinesq's approximation, the Tiwari and Das nanofluid model, and the mentioned assumptions, are formulated as presented in references [13 14].

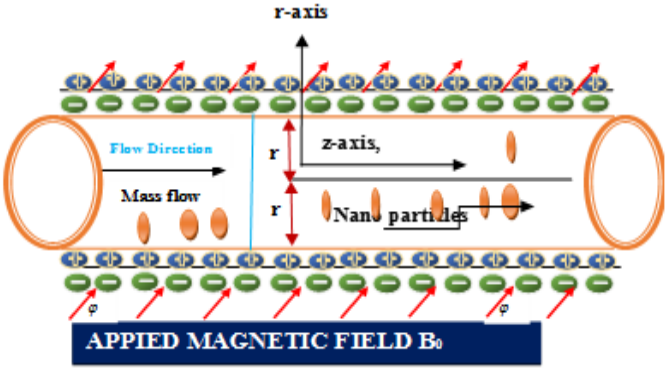

Figure 1: Physical schematic diagram of bifurcation flow channel in the presence of Electric Field

$$\left.\begin{aligned}&\rho_{nf}\frac{\partial \dot{u}_f(r,t)}{\partial \dot{t}}=-\frac{\partial \dot{p}}{\partial \dot{z}}+\mu_{nf}\left(1+\frac{1}{\beta}\right)\\&\left(\frac{\partial^2 \dot{u}_f(r,t)}{\partial\, \dot{r}^2}+\frac{1}{\dot{r}}\frac{\partial \dot{u}(r,t)}{\partial \dot{r}}\right)-\\&\delta_{nf}B_0{}^2\,\dot{u}_f(r,t)\sin\varphi+\\&\mathrm{KN}(u_p-u_f)-\frac{\mu_{nf}}{k_p}\dot{u}_f+\\&g(\beta\rho_{nf})(\mathrm{T}-\mathrm{T}_\infty)+\bar{\rho}_e\bar{E}_{\dot{z}}\end{aligned}\right\}\qquad(2)$$

$$m\frac{\partial \dot{u}_p}{\partial \dot{t}}=\mathrm{K}_s(\dot{u}_f-\dot{u}_p)\qquad(3)$$

$$\rho c_p\frac{\partial \dot{T}}{\partial \dot{t}}=\mathrm{K}_{nf}\left(\frac{\partial^2 \mathrm{T}}{\partial \dot{r}^2}+\frac{1}{\dot{r}}\frac{\partial \mathrm{T}}{\partial \dot{r}}\right)-\frac{d\dot{q}}{d\dot{r}}\qquad(4)$$

In the context of the study, various parameters are defined: $\dot{u}$ represents the velocity component along the z-axis, $\dot{t}$ represents the time parameter, $\partial\dot{p}/\partial\dot{z}$ signifies a pulsatile pressure gradient, $\beta=\mu_B\sqrt{2\pi_c}/\tau_y$ denotes the non-Newtonian Casson parameter, B_0 represents the applied magnetic field strength, k_p is the permeability constant, g is the gravitational acceleration, T represents the fluid temperature, and T_∞ represents the ambient temperature and

$$-\frac{d\dot{q}}{d\dot{r}}=4\alpha_2^2(T-T_\infty)$$

Additionally, the thermophysical properties related to Casson nanofluids are detailed in [15], with the nanofluid's viscosity being roughly equivalent to that of the base fluid containing spherical nanoparticles, as emphasized by Brinkman [16]. At the initial time (t = 0), both the fluid and the cylinder are at rest. As time progresses (t > 0), the fluid starts moving with a slip velocity at the boundary. Simultaneously, the cylinder's temperature rises from to the boundary temperature and then remains constant. The initial and boundary conditions for the problem are provided in references [16,17] therein.

$$\left.\begin{aligned}&\dot{u}_f(r,o)=0,\quad \mathrm{T}(r,0)=\mathrm{T}_\infty,\quad \dot{u}_p(r,o)=0,\qquad :r\in[0,r_0]\\&\dot{u}_f(\dot{r}_0,t)=\dot{u}_s,\quad T(\dot{r}_0,\dot{t})=T_w,\quad u_p(\dot{r}_0,\dot{t})=u_s\qquad ;t>0\end{aligned}\right\}\qquad(5)$$

where $\dot{u}_s$, s the slip velocity condition.

With the aid of electrostatics theory, the relationship between the net charge density $\bar{\rho}_e$ and the potential distribution $\dot{\psi}(\dot{r})$ is given by the expression;

$$\nabla^2\dot{\psi}(\dot{r})=\frac{1}{\dot{r}}\frac{\partial}{\partial \dot{r}}\left(\dot{r}\frac{\partial \dot{\psi}(\dot{r})}{\partial \dot{r}}\right)+\frac{1}{\dot{r}^2}\frac{\partial^2\dot{\psi}(\dot{r})}{\partial \dot{z}}=\frac{\bar{\rho}_e(\dot{r})}{\in}\qquad(6)$$

Known as the Boltzmann equation with the boundary condition and the net charge density

$$\dot{\psi}(1)=\dot{\psi}_w\ \text{and}\ \frac{\partial \dot{\psi}}{\partial \dot{r}}=0,\ \text{at}\ \dot{r}=0\qquad(7)$$

$$\bar{\rho}_e(\bar{r})=e_0\left(n^+-n^-\right)=\frac{-2z_0^2e_0^2n_0\dot{\psi}(\dot{r})}{k_gT_e}\qquad(8)$$

where $\in$ is the dielectric constant, $\bar{\psi}_w$ is the potential on the arterial wall, $z_0, n_0, e_0, k_g, T_e, n^+$ and n^- are the ion valence, concentration of ions, the electronic charge, the Boltzmann constant, the local absolute temperature of the fluid, the density number of cations and anions respectively. Using Debye-Huckel parameter

$$\dot{k}^2=\frac{2z_0^2e_0^2n_0\bar{\psi}(\bar{r})}{\in k_gT_e}\qquad(9)$$

and linearized the Boltzmann equation we get a potential equation as:

$$\frac{1}{\dot{r}}\frac{\partial}{\partial \dot{r}}\left(\dot{r}\frac{\partial \dot{\psi}(\dot{r})}{\partial \dot{r}}\right)=\dot{k}^2\dot{\psi}(\dot{r})\qquad(10)$$

The relevant dimensionless variables are stated as [18]:

$$\left.\begin{aligned} &, r=\frac{\dot{r}}{r_0}, u_f=\frac{\dot{u}_f}{u_0}, u_p=\frac{\dot{u}p}{u_0}, u_s=\frac{\dot{u}_s}{u_0}, \\ t=\frac{\dot{t}v}{r_0^{\,2}}\, z=\frac{\dot{z}}{r_0}, p=\frac{\dot{p}}{\mu u_0}, \theta=\frac{\mathrm{T}-\mathrm{T}_\infty}{\mathrm{T}_w-\mathrm{T}_\infty}, \psi=\frac{\dot{\psi}}{\psi_w}, \\ k=\frac{\dot{k}r_0}{u_0} \end{aligned}\right\} \quad (11)$$

The governing equations (2)-(4) and (10) along with conditions (5) and (7) are transformed into their dimensionless forms by utilizing the appropriate dimensionless variables in (Eq11), resulting in the following expressions.

$$\left.\begin{aligned} &\frac{\partial u_f}{\partial t}=-b_5\frac{\partial \rho}{\partial z}+b_6\beta_1\left(\frac{\partial u_f}{\partial r^2}+\frac{1}{r}\frac{\partial u_f}{\partial r}\right) \\ &+\mathrm{P}_c\left(u_p-u_f\right)- \\ &b_8\mathrm{M}\sin\varphi u_f+b_9 Gr\theta(r,t)-\frac{b_6}{Da}u_f \end{aligned}\right\} \quad (12)$$

$$P_m\frac{\partial u_f}{\partial u_t}=u_f-u_p \quad (13)$$

$$\left.\begin{aligned} &\frac{\partial\theta(r,t)}{\partial t}=\frac{b_3}{P_r}\left(\frac{\partial^2\theta(r,t)}{\partial r^2}+\frac{1}{r}\frac{\partial\theta(r,t)}{\partial r}\right) \\ &+\frac{R}{P_r}\theta(r,t) \end{aligned}\right\} \quad (14)$$

$$\frac{1}{r}\frac{\partial}{\partial r}\left(r\frac{\partial\psi(r)}{\partial r}\right)-k_e^2\psi(r)=0 \quad (15)$$

And the conditions:

$$\begin{aligned} &u_f(r,0)=0, \quad u_p(r,0)=0, \\ &\theta(r,0)=0 \quad ;r\in[0,1], \quad \psi(1)=1, \\ &u_f(1,t)=u_s, \quad u_\rho(1,t)=u_s, \\ &\theta(1,t)=1, \quad ;t>0, \ \frac{\partial\psi(0)}{\partial r}=0 \end{aligned} \quad (16)$$

Where;

$$\mathrm{M}=\frac{\delta_f r_0^2\mathrm{B}_0^2}{\mu_f}, Gr=\frac{g(\mathrm{B}_\mathrm{T})f(\mathrm{T}_w-\mathrm{T}_\infty)r_0^2}{v_f u_0},$$

$$P_r=\frac{v_f(\rho c_p)}{\mathrm{K}_f}, P_m=\frac{\mathrm{M}v_f}{r_0^2\mathrm{K}_s}, P_c=\frac{\mathrm{KN}r_0^2}{\mu},$$

$$\beta_1=\frac{1}{\beta_0}, \beta_0=1+\frac{1}{\beta}, R=\frac{4\alpha_2^2 r_0}{K_f}$$

Are Magnetic field parameter, Grashof mass number, Prandtl number, Particles mass parameter, Particle Concentration Parameter, Casson fluid parameter and Radiation parameter respectively.

Moreover, $-\frac{\partial\rho}{\partial z}=\mathrm{A}_0+\mathrm{A}_1\cos(wt)$ indicates the pulsatile pressure gradient that imitates the heart's pumping movement [18], where A_0 and A_1 are the constants of pulsatile amplitude, and ω is a pulsatile frequency. It is possible to rewrite the dimensionless momentum governing equation as:

$$\left.\begin{aligned} &\frac{\partial u_f}{\partial t}=b_5\left(\mathrm{A}_0+\mathrm{A}_1\cos(\omega t)\right)+ \\ &b_6\beta_1\left(\frac{\partial^2 u_f}{\partial r^2}+\frac{1}{r}\frac{\partial u_f}{\partial r}\right)+\rho_c\left(u_p-u_f\right) \\ &-\frac{b_6}{Da}u_f-b_8\mathrm{M}u_f \\ &+b_9 Gr\theta+k^2\psi(r) \end{aligned}\right\} \quad (17)$$

4. Problem Solution

Analyzing the blood flow in the slipping cylinder containing AuNPs requires the application of comprehensive techniques that integrate both Laplace and finite Hankel transforms. Specifically, when dealing with cylindrical domains, the finite Hankel transform offers substantial advantages, while the Laplace transform proves effective in handling initial-boundary values and transient issues. The reduction of partial differential equations (PDEs) leads to the emergence of ordinary differential equations (ODEs). By applying inverse transformations for both Laplace and finite Hankel, analytical results can be derived.

The resolution of equation (15) under the conditions specified in equation (16) is:

$$\psi(r)=\frac{I_0(k_e r)}{I_0(k)} \qquad \psi(r)=\frac{I_0(k_e r)}{I_0(k)} \quad (18)$$

where I_0 is the modified Bessel function of first kind and order zero. Initially, the Laplace transform technique is applied to the dimensionless form of the energy governing equation (Eq. 14) and the corresponding dimensionless conditions (Eq. 16), resulting in:

$$\left.\begin{aligned} s\bar{\theta}(r,s)&=\frac{b_3}{\rho_r}\left[\frac{d^2\bar{\theta}(r,s)}{dr^2}+\frac{1}{r}\frac{d\bar{\theta}(r,s)}{dr}\right] \\ &+Q_m\bar{\theta}(r,s) \end{aligned}\right\} \quad (19)$$

$$\bar{\theta}(1,s)=\frac{1}{s} \tag{20}$$

The Laplace transform of the function $\theta(r,t)$, denoted as $\bar{\theta}(r,s)$, is represented by, with the transformation variable being s. Subsequently, Eq. (19) undergoes transformation through the application of the zero-order finite Hankel transform, in conjunction with the condition (20), resulting in:

$$\bar{\theta}_H(r,s)=\frac{J_1(r_n)}{r_n}\left[\frac{1}{sP_r+b_3r_n^2-Q_m}\right] \tag{21}$$

Where $\bar{\theta}(r_n,s)=\int_0^1 r\bar{\theta}(r_n,s)J_0(rr_n)dr$ is the finite Hankel transform of the function $\theta(r,s)$and r_n with n = 0,1… are the positive roots of the equation $J_0(x)=0$, where J_0 is the Bessel function of the first kind and zero-order, and J_1 is the Bessel function of the first kind and first-order. Then, the result of simplifying Eq. (21) is:

$$\bar{\theta}_H(r\ ,s)=\frac{J_1(r_n)}{r_n}\left[\frac{1}{s}-\frac{1}{s+\left(\frac{b_3r_n^2-Q_m}{P_r}\right)}\right] \tag{22}$$

In the next step, Eq. (15) undergoes the inverse Laplace transforms, yielding:

$$\bar{\theta}_H(r,t)=\frac{J_1(r_n)}{r_n}\left[1-\exp\left(-\left(\frac{b_3r_n^2-Q_m}{P_r}\right)\right)\right] \tag{23}$$

Ultimately, the analytical solution for the temperature profiles (Eq. 23) is derived by applying the inverse finite Hankel transform, resulting in:

$$\theta(r,t)=1\begin{Bmatrix}-2\sum_{n=1}^{\infty}\frac{J_0(rr_n)}{r_nJ_1(r_n)}\frac{J_1(r_n)}{r_n}\\ \exp\left[\left(\frac{b_3r_n^2-Q_m}{P_r}\right)\right]\end{Bmatrix} \tag{24}$$

The dimensionless Nanoparticles concentration and momentum equations (13) and (17) and the associated conditions (8) are both solved by using the Laplace transform, which results in:

$$\bar{u}_p(r,s)=\frac{\bar{u}_f(r,s)}{sP_m+1} \tag{25}$$

$$s\bar{u}_f(r,s)=b_5\left(\frac{A_0}{s}+\frac{A_1s}{s^2+\omega^2}\right)+\left.\begin{aligned}&b_6\beta_1\left(\frac{d^2\bar{u}_f(r,s)}{dr^2}+\frac{1}{r^2}\frac{d\bar{u}_f(r,s)}{dr}\right)-\\&\frac{b_6}{Da}\bar{u}_f(r,s)-b_8M\sin\varphi\bar{u}_f(r,s)\\&+P_c\begin{pmatrix}\bar{u}_p(r,s)-\bar{u}_f(r,s)+\\b_9Gr\bar{\theta}(r,s)\end{pmatrix}+\frac{k^2\bar{\psi}(r)}{s}\end{aligned}\right\} \tag{26}$$

$$\bar{u}(1,s)=\frac{u_s}{s} \tag{27}$$

Following that, the method of finite Hankel transform of zero-order was employed to convert Laplace's partial differential equation (25)-(26) with the associated condition in (27) into an ordinary differential equation (ODE), denoted as:

$$s\bar{u}_{Hf}(r_n,s)=b_5\frac{J_1(r_n)}{r_n}\begin{pmatrix}\frac{A_0}{s}+\\\frac{A_1s}{s^2+\omega^2}\end{pmatrix}+\left.\begin{aligned}&b_6\beta_1\begin{bmatrix}\frac{r_nJ_1(r,n)}{s}u_s\\-r_n^2\bar{u}_{Hf}(r_n,s)\end{bmatrix}\\&-\frac{b_6}{Da}\bar{u}_{Hf}(r_n,s)\\&-b_8M\sin\varphi\bar{u}_{Hf}(r_n,s)+\\&P_c\begin{pmatrix}\bar{u}_{Hp}(r_n,s)-\\\bar{u}_{Hf}(r_n,s)+\\b_9Gr\theta_H(r_n,s)\end{pmatrix}+\\&\frac{k^2}{s}\frac{r_n}{r_n^2+k^2}J_1(r_n)\end{aligned}\right\} \tag{28}$$

$$\bar{u}_{Hp}(r_n,s)=\frac{\bar{u}_{Hf}(r_n,s)}{sP_m+1} \tag{29}$$

Where $\bar{u}_H(r_n,s)=\int_0^1 r\bar{u}(r_n,s)J_0(rr_n)dr$ is the finite Hankel transform of the function $u(r,s)$and r_n with n = 0,1… are the positive roots of the equation $J_0(x)=0$, where J_0 is the Bessel function of the first kind and zero-order, and J_1 is the Bessel function of the first kind and first-order.

On substituting (Eq,29) into (Eq,28) we the general momentum equation as;

$$\bar{u}_{Hf}(r,s)=\left[\begin{array}{l}\dfrac{b_5 J_1(r,n)}{r_n}\left[\dfrac{A_0}{s}+\dfrac{A_1 s}{s^2+\omega^2}\right]\\ +\dfrac{b_6\beta_1 J_1(r_n)}{s}u_s+\\ b_9 Gr\bar{\theta}_H(r,s)+\\ \dfrac{k^2}{s}\dfrac{r_n}{r_n^2+k^2}J_1(r_n)\end{array}\right]\frac{1}{s+b_{11}(n)} \qquad (30)$$

Similarly, the Nanoparticles concentration equation is obtained by integrating equation (30) and (29) as:

$$\bar{u}_{Hp}(r_n,s)=\frac{1}{sP_m+1}\left[\begin{array}{l}\dfrac{b_5 J_1(r,n)}{r_n}\left[\dfrac{A_0}{s}+\dfrac{A_1 s}{s^2+\omega^2}\right]\\ +\dfrac{b_6\beta_1 J_1(r_n)}{s}u_s+\\ b_9 Gr\bar{\theta}_H(r,s)+\\ \dfrac{k^2}{s}\dfrac{r_n}{r_n^2+k^2}J_1(r_n)\end{array}\right]\frac{1}{s+b_{11}(n)}$$

The inverse Laplace form of equation (23) and (24) with the aid of Gerby-Stefan's Algorithm and the results were simulated graphically with the aid of MATCARD software.

5. Results and Discussion

In this section, we showcase and analyze the numerical outcomes graphically generated through the utilization of Mathcad software. The simulations pertain to the electro-magneto-hydrodynamic blood flow within a small slip artery featuring an inclined magnetic field. The investigation takes into account the impacts of both the applied electric field and thermal radiation on the momentum and energy equations. To enhance our understanding of the physical model, we explore the influences of diverse physical parameters on the velocity profile, the equation governing Nano particles concentration, and the temperature distribution in the electro-magneto-hydrodynamic blood flow through a small slip artery with an inclined magnetic field, specifically in the context of breast cancer treatments.

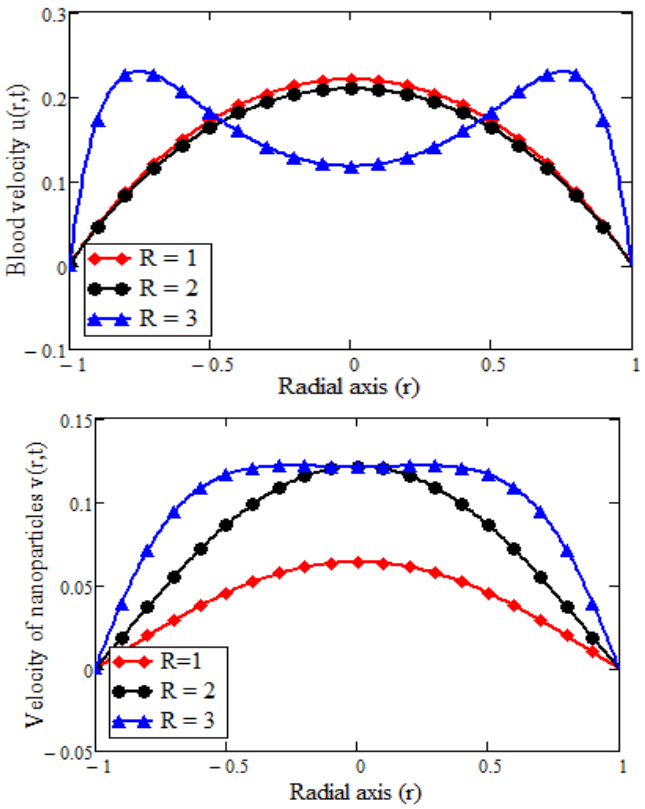

Figure 2: Variation of Blood velocity and Nanoparticles equations with radiation parameter

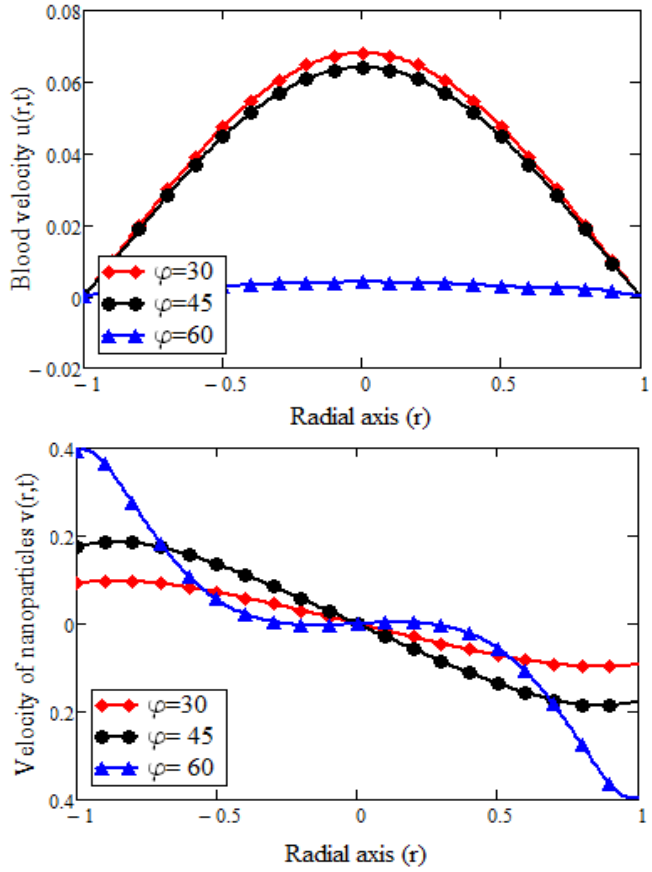

Figure 3: Variation of Blood velocity and Nanoparticles equations with an inclined Magnetic field

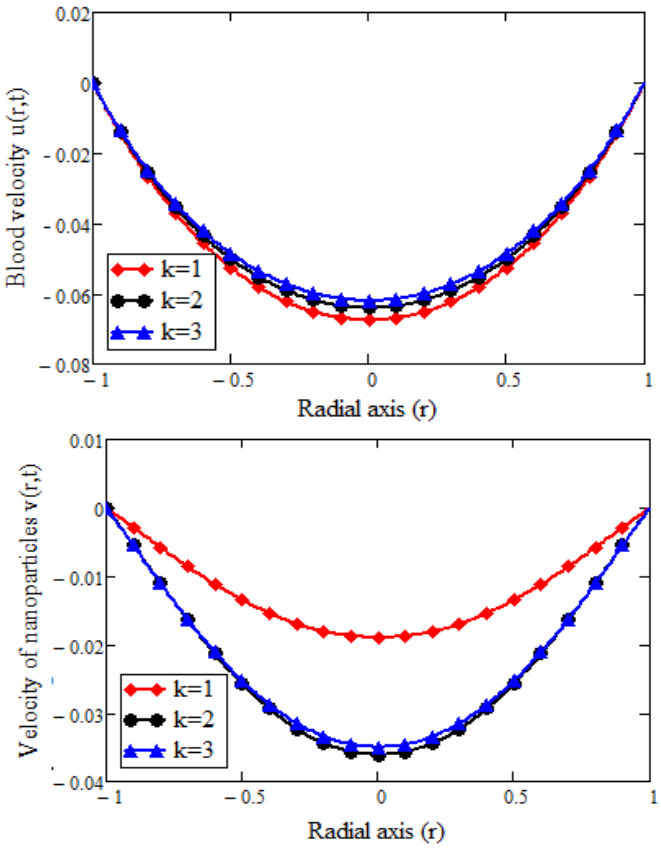

Figure 4: Variation of Blood velocity and Nanoparticles equations with electro-kinetic width

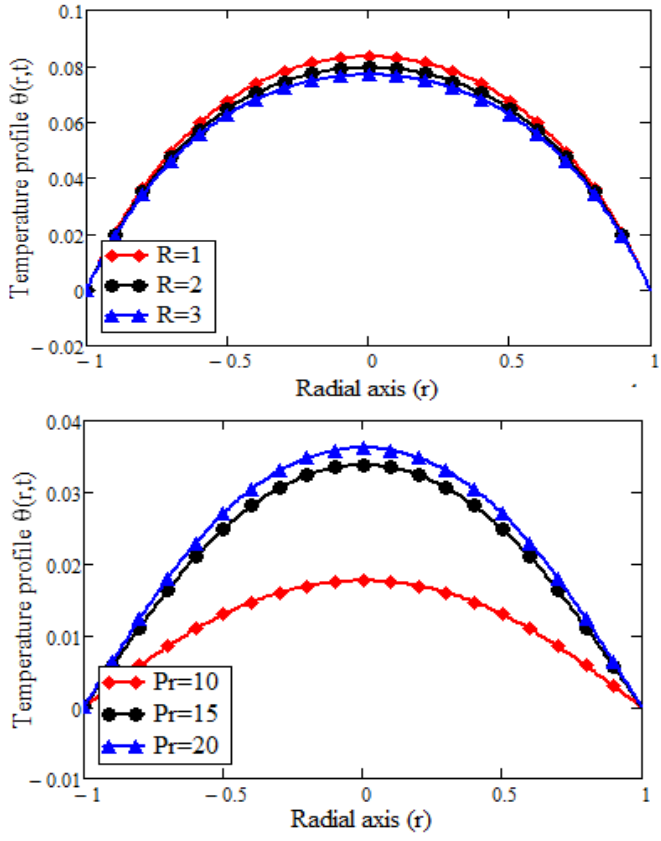

Figure 5: Variation of Temperature Profile Radiation Parameter and Prandtl Number respectively

Figures 2a and 2b were generated to depict the influence of the radiation parameter on fluid velocity and the equation governing Nanoparticles concentration, respectively. Both visualizations illustrate that an augmentation in the thermal radiation parameter results in a deceleration of blood flow. This phenomenon is ascribed to the presence of the applied electric field, effectively propelling the blood flow towards the cancerous region. Consequently, this mitigates or lessens the potential harm inflicted on neighbouring healthy cells by the administered radiation dosage. Figure 3 demonstrates that an increase in the angle of inclination leads to a reduction in both blood velocity and particle concentration. Notably, a significant decline in velocity is observed near the wall within the angle range of 300 to 450. This occurrence is attributed to the influence of the Lorentz force, establishing stability between the moving magnetic parameter and the inclined magnetic field. As a result, it counteracts the motion of the blood flow, causing a decrease in both velocity and particle concentration profiles within the affected region during cancer treatments.

In Figure 4a, a gradual rise in fluid velocity is observed with higher values of electrokinetic width, while Figure 4b exhibits the opposite trend. In the former, an increase in electrokinetic width may enhance electrokinetic forces, facilitating fluid movement. Conversely, in the latter, the rise in electrokinetic width leads to stronger interactions between particles, resulting in a reduction in fluid velocity during breast cancer treatments. Moving on to Figure 5a, higher values of the Radiation Parameter may indicate increased thermal radiation in the system, contributing to enhanced heat dissipation and a gradual decrease in fluid temperature. The impact of radiation on heat transfer mechanisms within the system plays a crucial role in this observed trend. Meanwhile, Figure 5b illustrates that the rise in fluid temperature with an increase in Prandtl number suggests more rapid heat diffusion in the system. A higher Prandtl number signifies a reduced ability of the fluid to conduct heat efficiently, potentially leading to elevated temperatures as the generated heat may not be efficiently dissipated, contributing to the observed trend.

6. Conclusion

In summary, the key findings of this study highlight the critical importance of comprehending blood flow dynamics for the development of effective therapeutic interventions, particularly in the realms of cancer treatment and drug delivery to cancer cell membranes. The pervasive impact of cardiovascular diseases on human health underscores the necessity of studying the circulatory system and blood flow to advance treatments for conditions like hypertension and myocardial infarction.

The utilization of mathematical models to investigate arterial blood flow under the influence of a magnetic field emerges as a valuable tool in simulating and understanding the intricate complexities of blood circulation. This approach holds immense potential for driving advancements in therapeutic

interventions, offering a more nuanced understanding of the physiological processes involved.

In conclusion, the presented findings emphasize the fundamental significance of unravelling the intricacies of blood flow and its profound implications for human health, particularly within the context of therapeutic development and the treatment of cardiovascular diseases. The incorporation of mathematical models into these investigations not only enhances our current understanding but also opens up promising avenues for future research. The dynamic simulations facilitated by mathematical models provide a robust platform for exploring blood flow under diverse conditions, laying the groundwork for innovative therapeutic strategies.

Recommendation for Further Studies:
Building upon the insights gained from this study, there are several promising areas for future research. Firstly, further investigations could delve into refining and expanding the mathematical models to incorporate additional factors that may influence blood flow dynamics, such as variations in vessel geometry and the impact of different non-Newtonian fluid models.

Additionally, exploring the potential applications of the developed models in the context of personalized medicine and patient-specific treatments could be an intriguing avenue. Tailoring therapeutic interventions based on individualized blood flow characteristics could lead to more targeted and effective treatments for cardiovascular diseases and cancer.

Furthermore, there is a need for experimental validations to corroborate the findings derived from mathematical simulations. Integrating experimental data with computational models would enhance the robustness of the conclusions and provide a more comprehensive understanding of blood flow phenomena.

In conclusion, future studies that build upon the foundation laid by this research should aim to refine models, explore personalized medicine applications, and incorporate experimental validations. These endeavours will contribute to advancing our understanding of blood flow dynamics and, consequently, foster innovative approaches to therapeutic interventions in the realms of cardiovascular diseases and cancer treatment.

Availability of Data and Materials
Not applicable

Conflict of interest
The authors declare that, there are no conflicts of interest for the study.

Funding
Tertiary Education Trust Fund (TETFund)

Authors' contributions statement: *All authors contributed equally to this work. They all read and approved the final version of the manuscript.*

Acknowledgment
This work was supported by Tertiary Education Trust Fund (TETFund).

Appendix:

$$b_1 = \frac{\mathrm{K}_s + 2\mathrm{K}_f - 2\phi\left(\mathrm{K}_f - \mathrm{K}_s\right)}{\mathrm{K}_s + 2\mathrm{K}_f + \phi\left(\mathrm{K}_f - \mathrm{K}_s\right)}$$

$$b_2 = \left(1-\phi\right) + \frac{\phi\left(\rho c_\rho\right)s}{\left(\rho c_\rho\right)f},$$

$$b_3 = \frac{b_1}{b_2}$$

$$b_4 = 1 + \frac{3\left(\delta - 1\right)\phi}{\left(\delta + 2\right) - \left(\delta - 1\right)}$$

$$b_5 = \frac{1}{\left(1-\phi\right) + \dfrac{\phi\rho_s}{\rho_f}},$$

$$b_6 = \frac{b_5}{\left(1-\phi\right)^{2.5}}$$

$$b_7 = \left(1-\phi\right) + \frac{\phi\left(\rho\beta_{\mathrm{T}}\right)_s}{\left(\rho\beta_{\mathrm{T}}\right)_f},$$

$$b_8 = b_4 b_5,$$

$$b_9 = b_5 b_7$$

$$b_{10} = \frac{b_6}{Da} + b_8\mathrm{M} - \frac{P_c}{sP_m + 1} + P_c,$$

$$b_{11}\left(n\right) = b_6\beta_1 r_n^2 + b_{10},$$

$$\delta = \frac{\delta_s}{\delta_f}$$

$$Q_m = \frac{R}{\mathrm{Pr}}$$

References

[1] R. Abdul and M. Yasir, "Electro-magneto- hydrodynamic flows of Burger fluids in cylindrical domains with time exponential memory," J. Appl. Comput. Mech., vol. **5,** no**. 4,** pp**.577-591, 2019.**

[2] M. Jain, G. C. Sharma, and R. Singh, "Mathematical modelling of blood flow in a stenosed artery under MHD effect through porous medium," Intern. J. Eng. Trans. B: Appl., vol**. 23,** no**. 3&4,** pp**. 243-251**, **2010**.

[3] M. Jain, G. C. Sharma, and R. Singh, "Mathematical modelling of blood flow in a stenosed artery under MHD effect through porous medium," Intern. J. Eng. Trans. B: Appl., vol**. 23,** no**. 3&4,** pp**. 243-251**, **2010**.

[4] N. Srivastava, "Analysis of flow characteristics of the blood flowing through an inclined tapered porous artery with mild stenosis under the influence of an inclined magnetic field," J. biophysics, vol**. 9,** pp**. 797-142**, **2014**.
[5] E. Omamoke, E. Amos, and E. Jatari, "Impact of thermal radiation and heat source on MHD blood flow with an inclined magnetic field in Treating Tumor and Low Blood Pressure," Asian, Res. J. Math, vol**. 16,** no**. 9,** pp**. 77–87, 2020**.
[6] J. Escandon, E. Jimenez, O. Hernandez, O. Bautista, and F. Mendez, "Transient electroosmotic flow of Maxwell Fluids in a slit microchannel with asymmtric zeta potentials," European J. Mechanics B/Fluids, vol**. 53,** pp**. 180-189**, **2015**.
[7] R. Ellahi and R. Arshad, "Analytical solutions for MHD flow in a thirdgrade fluid with variable viscosity," Math. Comput. Modell, vol**. 52,** no**. 9,** pp**. 1783–1793**, **2014**.
[8] I. A. Mirza, M. Abdulhameed, and S. Shafie, "Magnetohydrodynamic approach of non-newtonian blood flow with magnetic particles in stenosed artery," Appl. Math. Mech., vol**. 38,** no**. 3,** pp**. 379-392**, **2017**.
[9] O. Prakash, M. Singh, D. Kumar, and Y. K. Dwiredi, "A study of the effects of heat source on MHD blood flow through bifurcated arteries," American Institute of Physics Advances, vol. 1, 2011, 042128.
[10] D. Kumar, B. Satyanarayana, K. Rajesh, D.Narendra, and K. Sanjeev, "Application of heat source and chemical reaction in magnetohydrodynamic blood flow through permeable bifurcated arteries with inclined magnetic field in tumor treatments," Journal of results in applied Mathematics, vol.**10**, **100151,** pp**.1-13, 2021**.
[11] A. Isah, A. Musa, D. G. Yakubu, G. T. Adamu, A. Mohammed, A. Baba, S. Kadas, and A. Mahmood, "The impact of heatsource and chemical reaction on MHD blood flow through permeable bifurcated arteries with tilted magnetic field in tumor treatments, "Computer Methods in Biomechanics and Biomedical Engineering, vol.**10**, no.**2**, pp.**55- 84**,**2023.**
[12] F. W. Wan, A. Q. Mohamad, L. Y. Jiann, and S. Shafie, "Mathematical modelling of MHD Blood Flow with Gold Nanoparticles in Slip Small Arteries," J. Appl. Comput. Mech., vol.**10,** no**.1,** pp**.125-139**, **2023**.
[13] S. Maiti, S. Shaw, and G. C. Shit, "Fractional order model for thermochemical flow of blood with Dufour and Soret effects under magnetic and vibration environment," Colloids Surfaces B Biointerfaces, vol**.197**, **111395, 2021**.
[14]J. Raza, "Thermal radiation and slip effects on magnetohydrodynamic (MHD)stagnation point flow of Casson fluid over a convective stretching sheet," Propuls. Power Res., vol**.18**, pp**.138-146**, **2019.**
[15] K. Benhanifia, R. Lakhdar, M. Brahim, K. Al-Farhany, W. Jamshed, M. R. Ilias, and M. R. Eid, "Investigation of mixing viscoplastic fluid with a modified anchor impeller inside a cylindrical stirred vesselusing Casson–Papanastasiou model," Sci. Rep., vol.**12**, pp.**1–19, 2022.**
[16] A. Imtiaz, O. M. Foong, A. Khan, N. Ali, F. Khan, and I. Khan, "Generalized model of blood flow in a vertical tube with a suspension of gold nanomaterials: Applications in cancer therapy," Comput. Mater. Contin., vol. **65**, pp. **171–192**, **2020.**
[17] W. N. N. NoranuarMohamad, A. Q. Shafie, S. Khan, I. Jiann, L. Y. Ilias, and M. R. Non-coaxial rotation flow of MHD Casson nanofluid carbon nanotubes past a moving disk with porosity effect," Ain Shams Eng. Journal, vol**. 12**, pp**. 4099-4110**, **2021**,
[18] J. Mackolil, B. Mahanthesh, "Exact and statistical computations of radiated flow of nano and Casson fluids under heat and mass flux conditions," J. Comput. Des. Eng., vol.**6,** pp**. 593–605, 2019**.

